

Local magnetic properties of periodic nonuniform spin- $\frac{1}{2}$ XX chains

Oleg Derzhko^{1,2}, Johannes Richter³ and Oles' Zaburannyi¹

¹Institute for Condensed Matter Physics,

1 Svientsitskii Street, L'viv-11, 79011, Ukraine

²Chair of Theoretical Physics, Ivan Franko National University in L'viv,

12 Drahomanov Street, L'viv-5, 79005, Ukraine

³Institut für Theoretische Physik, Universität Magdeburg,

P.O. Box 4120, D-39016 Magdeburg, Germany

April 26, 2024

Abstract

Using the Jordan–Wigner fermionization, Green function approach and continued fractions we examine rigorously the local magnetizations and the local static susceptibilities of the spin- $\frac{1}{2}$ XX chain in a transverse field with regularly varying exchange interactions. We discuss our findings from a viewpoint of the strong-coupling approach.

PACS numbers: 75.10.-b

Keywords: spin- $\frac{1}{2}$ XX chain in a transverse field, periodically modulated exchange interactions, magnetization, susceptibility, strong-coupling approach

Postal addresses:

Dr. Oleg Derzhko (corresponding author)

Oles' Zaburannyi

Institute for Condensed Matter Physics

1 Svientsitskii Street, L'viv-11, 79011, Ukraine

tel/fax: (0322) 76 19 78

email: derzhko@icmp.lviv.ua

Prof. Johannes Richter

Institut für Theoretische Physik, Universität Magdeburg

P.O. Box 4120, D-39016 Magdeburg, Germany

tel: (0049) 391 671 8841

fax: (0049) 391 671 1217

email: Johannes.Richter@Physik.Uni-Magdeburg.DE

1 Introduction

In recent years there has been tremendous interest in the spin models of one-dimensional magnets because materials sciences have made a remarkable progress and a number of quasi-one-dimensional magnets have become available. On the one hand, the one-dimensional magnets may exhibit a wide variety of peculiar properties (e.g., gapless or gapped low-energy excitations, magnetization plateaus, spin-Peierls phases etc.). On the other hand, for the one-dimensional spin models specific theoretical tools can be applied (Jordan-Wigner fermionization, bosonization, Bethe ansatz etc.) and therefore a more comprehensive analysis can be performed. Although usually the Heisenberg model with modification is used to describe the properties of low-dimensional magnetic compounds, some of their generic features can be illustrated within the simpler framework of the XX model in a transverse field.

In the present paper we study the effects of regular modulation of the exchange interactions on the magnetization and static susceptibility examining for this purpose the local magnetic properties of the spin- $\frac{1}{2}$ XX chain in a transverse field. A model with the alternating exchange interactions arises while describing superlattices [1] or annealed “bond impurities” [2]. Recent study of the alternating quantum (Heisenberg) spin chain with experimental applications has been reported in [3]. Quantum spin chains with regularly modulated exchange interactions attract much attention because of the magnetization plateaus which can be realized in such chains. Oshikawa, Yamanaka and Affleck [4] considered a general quantum spin chain exhibiting rotational symmetry with respect to the direction of the applied uniform field and proposed the necessary condition for magnetization plateaus as $p(s - m) = \text{integer}$, where p is the period of chain, s is the spin value, m is the zero temperature magnetization per site. Much work has been done [5–9] to investigate magnetization plateaus in various quantum spin chains using approximate analytical approaches (mainly, bosonization plus renormalization group analysis or strong-coupling limit plus perturbation expansions) and numerical ones (mainly, exact diagonalization or density-matrix renormalization group techniques). On the other hand, for a simpler spin- $\frac{1}{2}$ XX chain the magnetization profiles can be calculated exactly for any finite period of nonuniformity p [10]. Moreover, as we shall show below, it is also possible to examine rigorously a nonuniversal behavior of the *local magnetizations* of such chains. In addition, we can calculate the *local static susceptibilities*. The local magnetic properties of quantum spin chains can be probed experimentally. Thus, the precise analysis of the NMR line shapes can yield the on-site magnetizations in the corresponding quasi-one-dimensional compounds [11, 12].

The paper is organized as follows. First we explain how the local magnetic properties of the regularly nonuniform spin- $\frac{1}{2}$ XX chain in a transverse field can be calculated exactly. Then we analyze the obtained results for the zero temperature magnetization profiles from a viewpoint of the strong-coupling limit. We show to what extent the exact zero temperature magnetization profiles can be reproduced within the framework of the strong-coupling approximation.

Further we discuss the temperature dependence of local static susceptibilities. We end up with a brief summary.

2 Continued fractions and the local magnetic properties

Consider a nonuniform spin- $\frac{1}{2}$ XX chain in a transverse field defined by the Hamiltonian

$$\begin{aligned} H &= \sum_{n=1}^N \Omega_n s_n^z + 2 \sum_{n=1}^N I_n (s_n^x s_{n+1}^x + s_n^y s_{n+1}^y) \\ &= \sum_{n=1}^N \Omega_n \left(s_n^+ s_n^- - \frac{1}{2} \right) + \sum_{n=1}^N I_n (s_n^+ s_{n+1}^- + s_n^- s_{n+1}^+). \end{aligned} \quad (1)$$

By applying the Jordan–Wigner transformation one comes to spinless fermions with the Hamiltonian

$$H = \sum_{n=1}^N \Omega_n \left(c_n^+ c_n - \frac{1}{2} \right) + \sum_{n=1}^N I_n (c_n^+ c_{n+1} - c_n c_{n+1}^+). \quad (2)$$

We shall be concerned with the local on-site magnetization $m_n = \langle s_n^z \rangle = \langle s_n^+ s_n^- \rangle - \frac{1}{2} = \langle c_n^+ c_n \rangle - \frac{1}{2}$ and the local on-site static susceptibility $\chi_n = \frac{\partial m_n}{\partial \Omega}$. Here the angular brackets denote the canonical thermodynamic average.

Let us introduce the Green functions [13] $G_{nm}^\mp(t) = \mp i \theta(\pm t) \langle \{c_n(t), c_m^\pm\} \rangle$, $G_{nm}^\mp(t) = \frac{1}{2\pi} \int_{-\infty}^{\infty} d\omega e^{-i\omega t} G_{nm}^\mp(\omega \pm i\epsilon)$, $\epsilon \rightarrow +0$, and note that for the model defined by Eq. (2) the following continued fraction representation for $G_{nn}^\mp \equiv G_{nn}^\mp(\omega \pm i\epsilon)$ holds

$$\begin{aligned} G_{nn}^\mp &= \frac{1}{\omega \pm i\epsilon - \Omega_n - \Delta_n^- - \Delta_n^+}, \\ \Delta_n^- &= \frac{I_{n-1}^2}{\omega \pm i\epsilon - \Omega_{n-1} - \frac{I_{n-2}^2}{\omega \pm i\epsilon - \Omega_{n-2} - \ddots}}, \\ \Delta_n^+ &= \frac{I_n^2}{\omega \pm i\epsilon - \Omega_{n+1} - \frac{I_{n+1}^2}{\omega \pm i\epsilon - \Omega_{n+2} - \ddots}}. \end{aligned} \quad (3)$$

For any finite period of varying of the Hamiltonian parameters Ω_n and I_n the continued fractions in Eq. (3) become periodic and can be evaluated by solving quadratic equations. As a result one gets the exact expressions for G_{nn}^\mp , $\langle c_n^+ c_n \rangle = \mp \frac{1}{\pi} \int_{-\infty}^{\infty} d\omega \frac{\text{Im} G_{nn}^\mp}{e^{\beta\omega} + 1}$, and hence for m_n and χ_n . Introducing the “local” density of states $\rho_n(\omega) = \mp \frac{1}{\pi} \text{Im} G_{nn}^\mp$ the formulas for m_n and χ_n can be rewritten as follows

$$m_n = -\frac{1}{2} \int_{-\infty}^{\infty} d\omega \rho_n(\omega) \tanh \frac{\beta\omega}{2}, \quad (4)$$

$$\chi_n = -\frac{\beta}{4} \int_{-\infty}^{\infty} d\omega \frac{\rho_n(\omega)}{\cosh^2 \frac{\beta\omega}{2}}. \quad (5)$$

Here $\beta = \frac{1}{kT}$ is the reciprocal temperature. Knowing the local quantities $\rho_n(\omega)$, m_n and χ_n one immediately gets the (total) density of states $\rho(\omega) = \frac{1}{N} \sum_{n=1}^N \rho_n(\omega)$ and the (total) magnetization and static susceptibility $m = \frac{1}{N} \sum_{n=1}^N m_n$ and $\chi = \frac{1}{N} \sum_{n=1}^N \chi_n$, respectively.

Following the procedure outlined above for the calculation of $\rho_n(\omega)$ (some further details can be found in [10] where, however, only the total density of states $\rho(\omega)$ was considered) one can easily derive $\rho_n(\omega)$ for chains provided the period is not too long. For example, for a chain of period 3 one finds

$$\rho_n(\omega) = \begin{cases} \frac{1}{\pi} \frac{|\mathcal{Y}_n(\omega)|}{\sqrt{\mathcal{C}(\omega)}}, & \text{if } \mathcal{C}(\omega) > 0, \\ 0, & \text{otherwise,} \end{cases} \quad (6)$$

$$\mathcal{Y}_n(\omega) = (\omega - \Omega_{n+1})(\omega - \Omega_{n+2}) - I_{n+1}^2,$$

$$\mathcal{C}(\omega) = 4I_1^2 I_2^2 I_3^2 - (I_1^2(\omega - \Omega_3) + I_2^2(\omega - \Omega_1) + I_3^2(\omega - \Omega_2) - (\omega - \Omega_1)(\omega - \Omega_2)(\omega - \Omega_3))^2$$

$$= - \prod_{j=1}^6 (\omega - c_j),$$

where c_j are the six roots of the equation $\mathcal{C}(\omega) = 0$. For a chain of period 4 the corresponding result is

$$\rho_n(\omega) = \begin{cases} \frac{1}{\pi} \frac{|\mathcal{W}_n(\omega)|}{\sqrt{\mathcal{D}(\omega)}}, & \text{if } \mathcal{D}(\omega) > 0, \\ 0, & \text{otherwise,} \end{cases} \quad (7)$$

$$\mathcal{W}_n = (\omega - \Omega_{n+1})(\omega - \Omega_{n+2})(\omega - \Omega_{n+3}) - I_{n+1}^2(\omega - \Omega_{n+3}) - I_{n+2}^2(\omega - \Omega_{n+1}),$$

$$\mathcal{D}(\omega) = 4I_1^2 I_2^2 I_3^2 I_4^2 - ((\omega - \Omega_1)(\omega - \Omega_2)(\omega - \Omega_3)(\omega - \Omega_4)$$

$$- I_1^2(\omega - \Omega_3)(\omega - \Omega_4) - I_2^2(\omega - \Omega_1)(\omega - \Omega_4)$$

$$- I_3^2(\omega - \Omega_1)(\omega - \Omega_2) - I_4^2(\omega - \Omega_2)(\omega - \Omega_3)$$

$$+ I_1^2 I_3^2 + I_2^2 I_4^2)^2 = - \prod_{j=1}^8 (\omega - d_j),$$

where d_j are the eight roots of the equation $\mathcal{D}(\omega) = 0$. The analytical calculation of $\rho_n(\omega)$ for chains of larger periods can be easily implemented on a small computer (see the results for periods 6 and 12 presented below).

3 Magnetization: exact results

Let us discuss the local magnetic properties of the spin model (1) induced by regular nonuniformity. In what follows we restrict ourselves to a case of the uniform field $\Omega_n = \Omega$ and assume that $I_n = I(1 + \delta_n)$ where δ_n is taken either in the form $\delta_n = \delta(\delta_{n,1} - \delta_{n,2} + \delta_{n,1+p} - \delta_{n,2+p} + \delta_{n,1+2p} - \delta_{n,2+2p} + \dots)$ or in the form $\delta_n = -\delta \cos \frac{2\pi n}{p}$. The parameter δ controls the deviation from uniformity and the parameter p is the period of modulation of the exchange interactions. The modulation of exchange interactions may be interpreted as a result of the lattice distortion. For example, the first ansatz for δ_n corresponds to a displacement of the second site towards the first one, of the $(p+2)$ th site towards the $(p+1)$ th one and so on. The second ansatz corresponds to the displacements of sites giving by cosine with period p . Some relevant lattice configurations for $p = 3, 4, 6, 12$ are shown in Fig. 1. In our illustrations presented below we

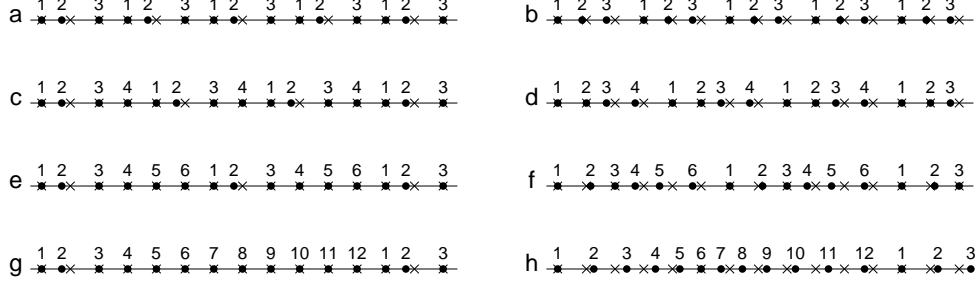


Figure 1: Lattice distortions of the form $\delta_n = \delta(\delta_{n,1} - \delta_{n,2} + \delta_{n,1+p} - \delta_{n,2+p} + \delta_{n,1+2p} - \delta_{n,2+2p} + \dots)$ (a, c, e, g) and of the form $\delta_n = -\delta \cos \frac{2\pi n}{p}$ (b, d, f, h) for $p = 3$ (a, b), $p = 4$ (c, d), $p = 6$ (e, f) and $p = 12$ (g, h).

put for concreteness $I = 1$, $\delta = 0.6$ (except Figs. 4, 5 where δ varies from 0.3 to 0.999).

In Fig. 2 the zero temperature dependences of local magnetizations m_n on field Ω are depicted. Similarly to the total magnetization m , the local magnetizations m_n in regularly alternating XX chains exhibit a step-like dependence on the applied field. From the mathematical point of view this is the consequence of a splitting of the initial fermion band ($\rho_n(\omega) = \frac{1}{\pi} \frac{1}{\sqrt{4I^2 - (\omega - \Omega)^2}}$ if $\Omega - 2|I| < \omega < \Omega + 2|I|$ and $\rho_n(\omega) = 0$ otherwise) into several subbands, the edges of which are determined by the roots of equations $\mathcal{C}(\omega) = 0$ (6), $\mathcal{D}(\omega) = 0$ (7), etc.. As a result the zero temperature dependence m_n vs. Ω [as well as m vs. Ω] must be composed of sharply increasing parts (as can be seen from Eq. (4) they appear when $\omega = 0$ remains inside a subband while Ω increases) separated by the horizontal parts (they appear when $\omega = 0$ remains outside a subband while Ω increases). The characteristic fields at which the horizontal parts of the dependences m_n vs. Ω begin and end up (and therefore the plateau lengths) are the same for all m_n and coincide with the values of such fields for m , since in all the cases those fields are determined by the roots of equations $\mathcal{C}(\omega) = 0$, $\mathcal{D}(\omega) = 0$, etc.. However, the heights of plateaus m_n are essentially site-dependent quantities. Moreover, the values of m_n depend on δ . This is in contrast to the behavior of m , since the possible values of m are universal and do not depend on details of the intersite exchange interactions. As can be seen, for example, in Fig. 2b for the lattice shown in Fig. 1b the magnetization at site 2 in weak and in moderate fields is always smaller than the magnetizations at sites 1 and 3 and its value depend on δ (compare the results for $\delta = 0.6$ seen in Figs. 2a, 2b, 2e and for $\delta = 1$ presented below). On the other hand, the sequence $m_{n_1} \leq m_{n_2} \leq \dots \leq m_{n_p}$ may depend on the value of the applied field Ω as can be seen in Fig. 2e (and Figs. 2g, 2h). For example, for the chain shown in Fig. 1e $-m_1 < -m_4 < -m_2 < -m_5 < -m_6 < -m_3$ for $0.7037 \dots \leq \Omega \leq 1.3578 \dots$ but $-m_1 < -m_2 < -m_6 < -m_5 < -m_4 < -m_3$ for $1.5884 \dots \leq \Omega \leq 2.0139 \dots$. The mentioned property is also visible in Fig. 3 where the zero temperature magnetization profiles along chains for various fields are displayed. Moreover, the sequence $m_{n_1} \leq m_{n_2} \leq \dots \leq m_{n_p}$ for a certain Ω may depend on δ as can be seen in Fig. 4. The results presented in Fig. 2 (3) indicate a relation between the periodically modulated

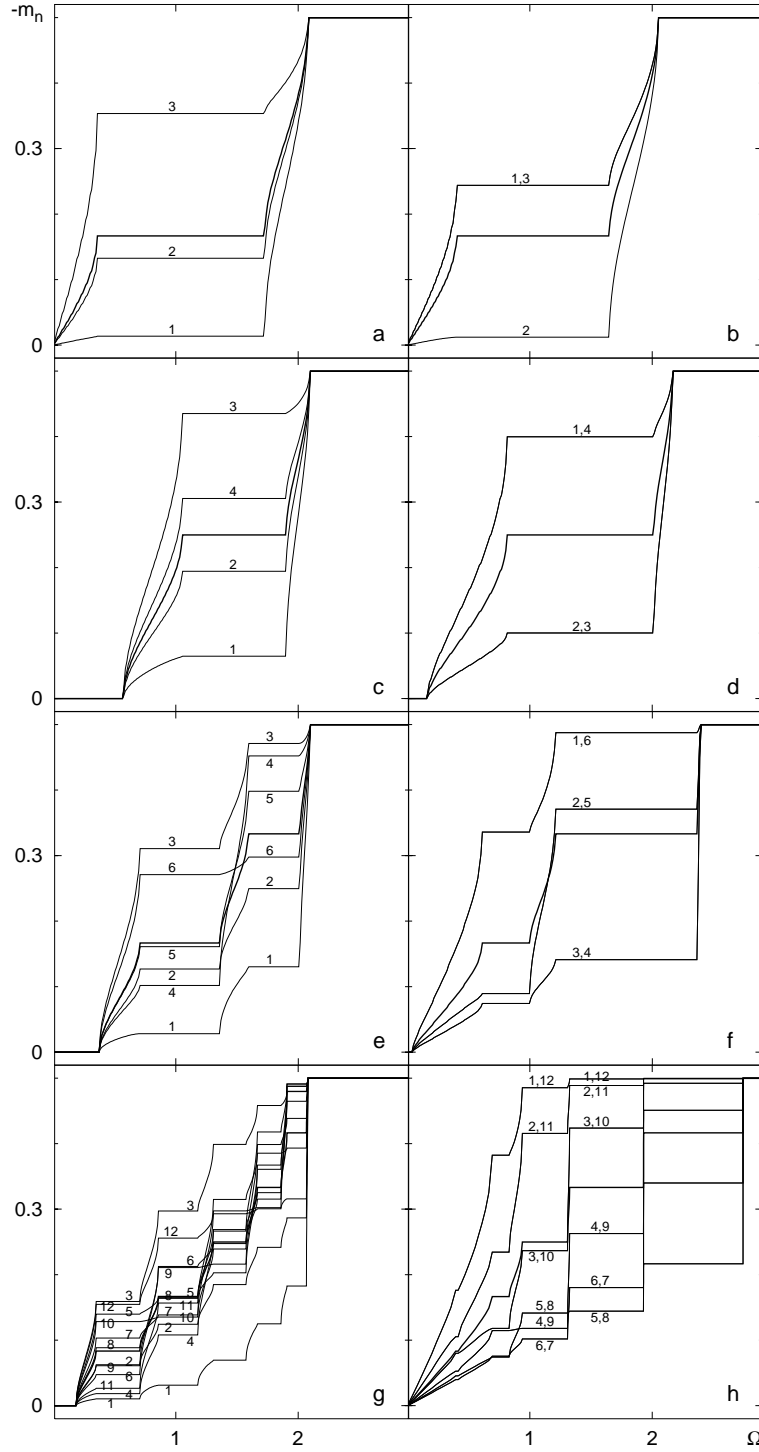


Figure 2: Local magnetizations m_n vs. field Ω at zero temperature $\beta = \infty$ for the chains shown in Fig. 1 ($I = 1$, $\delta = 0.6$). Panel a corresponds to the chain shown in Fig. 1a, panel b corresponds to the chain shown in Fig. 1b, and so on; the curve denoted by n presents the local magnetization m_n ; the bold curves present m .

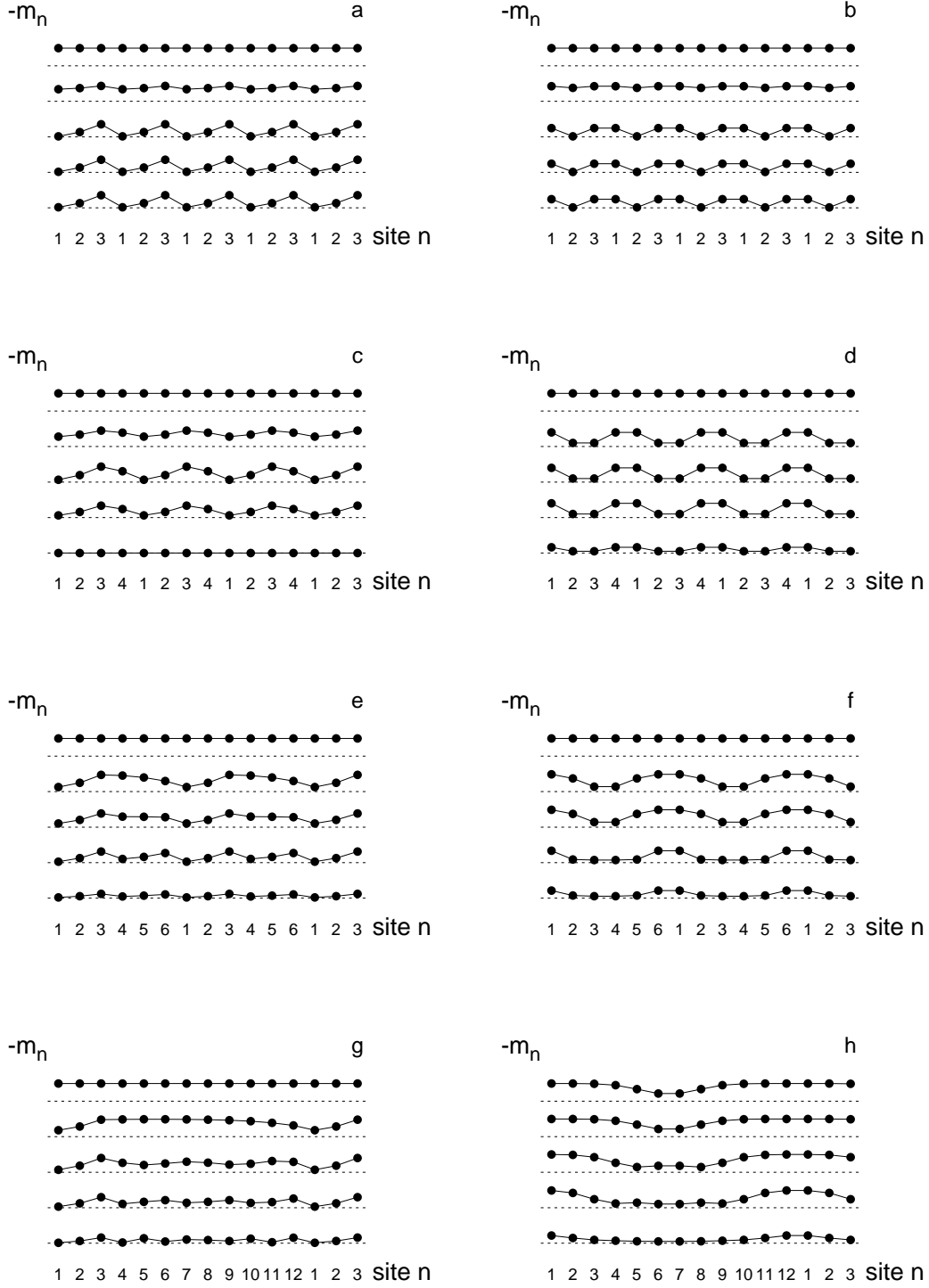


Figure 3: Zero-temperature magnetization profiles $\{m_n\}$ at $\Omega = 0.5, 1, 1.5, 2, 2.5$ (from bottom to top) for the chains shown in Fig. 1 ($I = 1$, $\delta = 0.6$). Dashed lines indicate $m_n = 0$. Panel a corresponds to the chain shown in Fig. 1a, panel b corresponds to the chain shown in Fig. 1b, and so on.

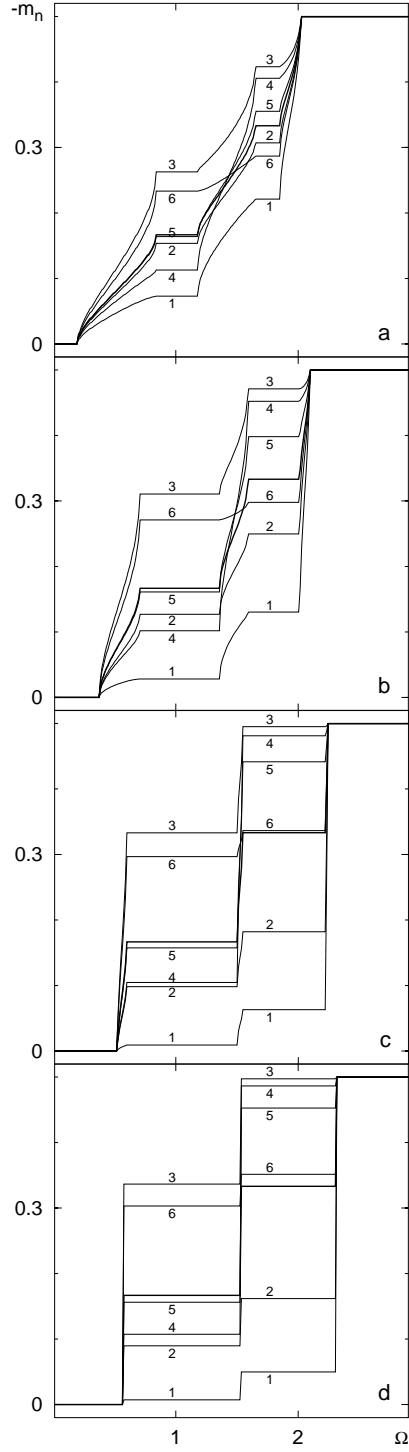


Figure 4: Local magnetizations m_n vs. field Ω at zero temperature for the chain shown in Fig. 1e for $\delta = 0.3$ (a), 0.6 (b), 0.9 (c), 0.999 (d) ($I = 1$).

exchange interactions [or lattice distortion] and magnetization profiles at different sites (magnetization profiles along a chain for various fields), which for the considered spin- $\frac{1}{2}$ XX chain in a transverse field can be traced rigorously. Such correspondence may be of experimental importance. Thus, the NMR spectra yield the distribution of the local magnetization (see, for example, [11, 12]). In particular, such analysis was performed to confirm that the lattice modulation in the incommensurate phase in CuGeO_3 has the form of a soliton lattice [11].

4 Magnetization: strong-coupling approximation

Although we are able to calculate the magnetization profiles for the periodic nonuniform spin- $\frac{1}{2}$ XX chain exactly it is worth to consider those results from a viewpoint of the strong-coupling approximation, which was exploited in a number of papers devoted to spin chains [8] and ladders [9]. On the one hand, by turning to the strong-coupling limit, we can understand better the magnetization processes at zero temperature $\beta = \infty$ having a physical picture in terms of spins rather than in terms of Jordan-Wigner fermions. On the other hand, we can use the exact results as a testing ground to see how the approximate approach works. In the strong-coupling limit we put $\delta = 1$. In such a limiting case the chain of period p splits into noninteracting clusters each consisting of p sites. The zero temperature local magnetization in such limit is given by $m_n = \langle GS | s_n^z | GS \rangle$ where $|GS\rangle$ is the ground state eigenvector of the cluster Hamiltonian. The magnetization plateaus arise due to a change of the ground state with varying of the field.

Consider, for example, the chain of $p = 3$ shown in Fig. 1a. The relevant 3-site cluster Hamiltonian has the following eigenvectors and eigenvalues

$$\begin{aligned} |1\rangle &= \frac{1}{\sqrt{10}} |\downarrow_1 \downarrow_2 \uparrow_3\rangle + \frac{2}{\sqrt{10}} |\downarrow_1 \uparrow_2 \downarrow_3\rangle - \frac{1}{\sqrt{2}} |\uparrow_1 \downarrow_2 \downarrow_3\rangle, & |2\rangle &= \frac{1}{\sqrt{10}} |\uparrow_1 \uparrow_2 \downarrow_3\rangle + \frac{2}{\sqrt{10}} |\uparrow_1 \downarrow_2 \uparrow_3\rangle - \frac{1}{\sqrt{2}} |\downarrow_1 \uparrow_2 \uparrow_3\rangle, \\ |3\rangle &= |\downarrow_1 \downarrow_2 \downarrow_3\rangle, & |4\rangle &= \frac{2}{\sqrt{5}} |\downarrow_1 \downarrow_2 \uparrow_3\rangle - \frac{1}{\sqrt{5}} |\downarrow_1 \uparrow_2 \downarrow_3\rangle, \\ |5\rangle &= \frac{2}{\sqrt{5}} |\uparrow_1 \uparrow_2 \downarrow_3\rangle - \frac{1}{\sqrt{5}} |\uparrow_1 \downarrow_2 \uparrow_3\rangle, & |6\rangle &= |\uparrow_1 \uparrow_2 \uparrow_3\rangle, \\ |7\rangle &= \frac{1}{\sqrt{10}} |\downarrow_1 \downarrow_2 \uparrow_3\rangle + \frac{2}{\sqrt{10}} |\downarrow_1 \uparrow_2 \downarrow_3\rangle + \frac{1}{\sqrt{2}} |\uparrow_1 \downarrow_2 \downarrow_3\rangle, & |8\rangle &= \frac{1}{\sqrt{10}} |\uparrow_1 \uparrow_2 \downarrow_3\rangle + \frac{2}{\sqrt{10}} |\uparrow_1 \downarrow_2 \uparrow_3\rangle + \frac{1}{\sqrt{2}} |\downarrow_1 \uparrow_2 \uparrow_3\rangle, \end{aligned} \quad (8)$$

$$\begin{aligned} E_1 &= -\frac{1}{2}\Omega - \sqrt{5}I, & E_2 &= \frac{1}{2}\Omega - \sqrt{5}I, & E_3 &= -\frac{3}{2}\Omega, & E_4 &= -\frac{1}{2}\Omega, \\ E_5 &= \frac{1}{2}\Omega, & E_6 &= \frac{3}{2}\Omega, & E_7 &= -\frac{1}{2}\Omega + \sqrt{5}I, & E_8 &= \frac{1}{2}\Omega + \sqrt{5}I, \end{aligned} \quad (9)$$

respectively. As follows from Eq. (9) for $0 < \Omega < \sqrt{5}I$ the ground state is $|1\rangle$ and therefore according to Eq. (8) $m_1 = 0$, $m_2 = -\frac{1}{10}$, $m_3 = -\frac{2}{5}$, and $m = -\frac{1}{6}$, that agreeing with the results for $\delta = 0.6$ plotted in Fig. 2a. If Ω exceeds $\sqrt{5}I$ then the ground state is $|3\rangle$ and according to Eq. (8) one gets $m_1 = m_2 = m_3 = m = -\frac{1}{2}$. Similar arguments applied to the chain shown in Fig. 1b yield $m_1 = m_3 = -\frac{1}{4}$, $m_2 = 0$ if $0 < \Omega < \frac{3}{\sqrt{2}}I$ and $m_1 = m_2 = m_3 = -\frac{1}{2}$ if $\Omega > \frac{3}{\sqrt{2}}I$.

Let us consider further the chain of $p = 6$ shown in Fig. 1e. The eigenvalues and the eigenvectors of the relevant 6-site cluster Hamiltonian can be easily found numerically. Thus, the eigenvector $|S^z = -1\rangle$, i.e. with the expectation value of $S^z = s_1^z + \dots + s_6^z$ equals to -1 , which yields the lowest energy in this sector of S^z , is

$$\begin{aligned}
|S^z = -1\rangle = & -0.16|\downarrow_1\downarrow_2\downarrow_3\downarrow_4\uparrow_5\uparrow_6\rangle + 0.21|\downarrow_1\downarrow_2\downarrow_3\uparrow_4\downarrow_5\uparrow_6\rangle - 0.14|\downarrow_1\downarrow_2\uparrow_3\downarrow_4\downarrow_5\uparrow_6\rangle \\
& + 0.23|\downarrow_1\uparrow_2\downarrow_3\downarrow_4\downarrow_5\uparrow_6\rangle - 0.23|\uparrow_1\downarrow_2\downarrow_3\downarrow_4\downarrow_5\uparrow_6\rangle - 0.07|\downarrow_1\downarrow_2\downarrow_3\uparrow_4\uparrow_5\downarrow_6\rangle \\
& + 0.06|\downarrow_1\downarrow_2\uparrow_3\downarrow_4\uparrow_5\downarrow_6\rangle - 0.38|\downarrow_1\uparrow_2\downarrow_3\downarrow_4\uparrow_5\downarrow_6\rangle + 0.41|\uparrow_1\downarrow_2\downarrow_3\downarrow_4\uparrow_5\downarrow_6\rangle \\
& - 0.02|\downarrow_1\downarrow_2\uparrow_3\uparrow_4\downarrow_5\downarrow_6\rangle + 0.39|\downarrow_1\uparrow_2\downarrow_3\uparrow_4\downarrow_5\downarrow_6\rangle - 0.44|\uparrow_1\downarrow_2\downarrow_3\uparrow_4\downarrow_5\downarrow_6\rangle \\
& - 0.25|\downarrow_1\uparrow_2\uparrow_3\downarrow_4\downarrow_5\downarrow_6\rangle + 0.28|\uparrow_1\downarrow_2\uparrow_3\downarrow_4\downarrow_5\downarrow_6\rangle - 0.06|\uparrow_1\uparrow_2\downarrow_3\downarrow_4\downarrow_5\downarrow_6\rangle,
\end{aligned} \tag{10}$$

whereas the eigenvector $|S^z = -2\rangle$, i.e. with the expectation value of S^z equals to -2 , which yields the lowest energy for given S^z , is

$$\begin{aligned}
|S^z = -2\rangle = & 0.38|\downarrow_1\downarrow_2\downarrow_3\downarrow_4\downarrow_5\uparrow_6\rangle - 0.22|\downarrow_1\downarrow_2\downarrow_3\downarrow_4\uparrow_5\downarrow_6\rangle + 0.12|\downarrow_1\downarrow_2\downarrow_3\uparrow_4\downarrow_5\downarrow_6\rangle \\
& - 0.05|\downarrow_1\downarrow_2\uparrow_3\downarrow_4\downarrow_5\downarrow_6\rangle + 0.58|\downarrow_1\uparrow_2\downarrow_3\downarrow_4\downarrow_5\downarrow_6\rangle - 0.67|\uparrow_1\downarrow_2\downarrow_3\downarrow_4\downarrow_5\downarrow_6\rangle
\end{aligned} \tag{11}$$

(only two digits after decimal point are preserved in the expansion coefficients in Eqs. (10), (11)). Calculating the expectation values of s_n^z with the help of Eq. (10) and Eq. (11) one immediately finds that $\langle S^z = -1 | s_4^z | S^z = -1 \rangle > \langle S^z = -1 | s_6^z | S^z = -1 \rangle$ and $\langle S^z = -2 | s_4^z | S^z = -2 \rangle < \langle S^z = -2 | s_6^z | S^z = -2 \rangle$ just what was observed in Fig. 2e, however, for finite $\delta = 0.6$. A validity of the strong-coupling limit predictions (which are exact at $\delta = 1$) can be estimated from Fig. 4 where we plot the exact zero temperature magnetization profiles for the chain shown in Fig. 1e with δ varying from 0.3 to 0.999.

The results of the strong-coupling limit may be used to obtain the approximate zero temperature magnetization profiles when δ is slightly less than 1. Consider, for example, the chain of $p = 3$ shown in Fig 1a. The Hamiltonian can be naturally split into a sum of 3-site cluster Hamiltonians (main part) and a part describing the inter-cluster interaction (perturbation). Only the two lowest levels of the 3-site cluster Hamiltonian should be taken into account to describe the zero temperature magnetization profiles in the region between $m = -\frac{1}{6}$ and $m = -\frac{1}{2}$. We assume $\Omega \geq 0$ and hence the lowest relevant levels are $|1\rangle$ and $|3\rangle$. Introducing spin $\frac{1}{2}$ operators σ^α attached to each cluster which act as $\sigma^z|1\rangle = -\frac{1}{2}|1\rangle$, $\sigma^z|3\rangle = \frac{1}{2}|3\rangle$ etc. one can find that the zero temperature magnetization profiles can be calculated with the help of the Hamiltonian of the uniform spin- $\frac{1}{2}$ XX chain in a transverse field

$$H = \sum_{l=1}^L \left(-\Omega - \frac{1}{2} \sqrt{1 + (1 + \delta)^2} I + \left(\sqrt{1 + (1 + \delta)^2} I - \Omega \right) \sigma_l^z \right) + \frac{1 - \delta^2}{1 + (1 + \delta)^2} I \sum_{l=1}^L (\sigma_l^x \sigma_{l+1}^x + \sigma_l^y \sigma_{l+1}^y). \tag{12}$$

Moreover, the spin operators at sites s_n^z are expressed through σ^z as follows

$$\begin{aligned} s_1^z &= -\frac{1}{4} - \frac{1}{2}\sigma^z, \\ s_2^z &= -\frac{2 + (1 + \delta)^2}{4(1 + (1 + \delta)^2)} - \frac{(1 + \delta)^2}{2(1 + (1 + \delta)^2)}\sigma^z, \\ s_3^z &= -\frac{1 + 2(1 + \delta)^2}{4(1 + (1 + \delta)^2)} - \frac{1}{2(1 + (1 + \delta)^2)}\sigma^z. \end{aligned} \quad (13)$$

Dotted curves in Fig. 5 show how this effective Hamiltonian works while δ deviates from 1. We can compare the exact and approximate results. As δ decreases the strong-coupling approximation predictions for the values of m_n , characteristic fields, and detailed shape of profiles start to differ noticeably from the exact results. However, even for $\delta = 0.6$ (Fig. 5b) the strong-coupling approximation yields a reasonably good quantitative picture of the magnetization process in the region between $m = -\frac{1}{6}$ and $m = -\frac{1}{2}$. Evidently, for small δ (Fig. 5a) the strong-coupling approach becomes worse and fails in the uniform limit $\delta \rightarrow 0$ as can be seen from Eq. (13). Obviously, the strong-coupling approach can be used for other chains with regularly modulated exchange interactions (e.g. the Heisenberg chain), for which there are no exact results and the results presented in Fig. 5 may be of use to estimate the accuracy of the strong-coupling approximation.

5 Susceptibility

Last let us turn to the local static susceptibilities (5). In Fig. 6 the temperature dependences of χ_n at $\Omega = 0$ are displayed. Such dependences are different at various sites. For example, the spin at site 2 of the chain shown in Fig. 1b at low temperature shows little response to the applied field in contrast to spins at sites 1 and 3 (see Fig. 6b). It can be also noted that some spins in a nonuniform chain (e.g., the spins at sites 5 – 8 for the chain shown in Fig. 1h) may exhibit almost a temperature-independent static susceptibility. Usually for the gapped (gapless) at $\Omega = 0$ chains shown in Figs. 1c, 1d, 1e, 1f, 1g (Figs. 1a, 1b, 1h) the low-temperature behavior of χ_n and χ differs only in quantitative details. However, in special cases we can observe a qualitative difference. Thus, the temperature behavior of the static susceptibility for a gapless chain mostly increases from a finite value to a maximum and then decreases inversely proportionally to temperature, whereas, for example, the local susceptibility at site 1 (2) of the chain shown in Fig. 1a (1b) exhibits a different behavior: as the temperature increases it decreases achieving a minimum at a finite temperature and then increases approaching the high-temperature asymptotic.

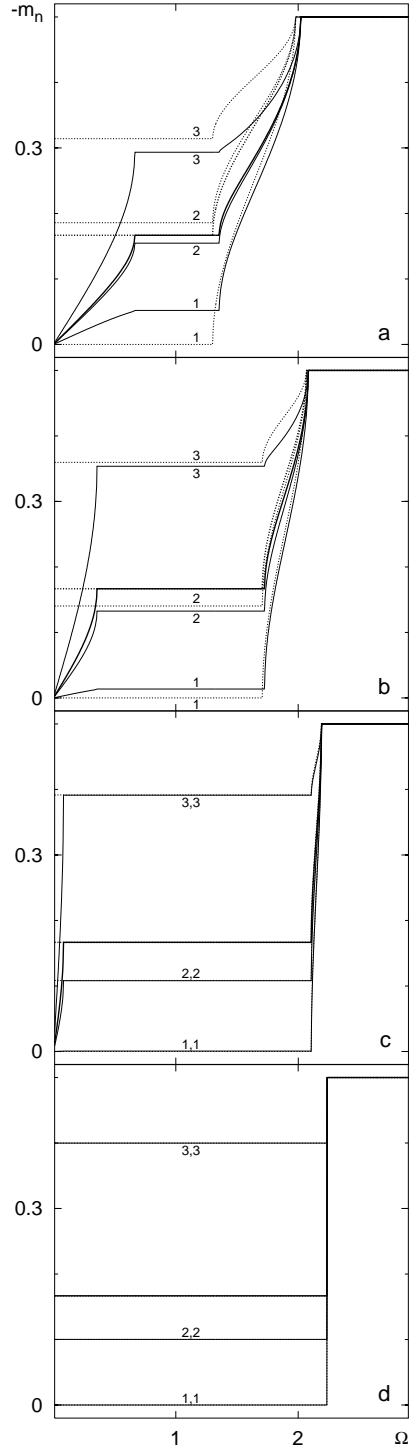


Figure 5: Local magnetizations m_n vs. field Ω at zero temperature for the chain shown in Fig. 1a for $\delta = 0.3$ (a), 0.6 (b), 0.9 (c), 0.999 (d) ($I = 1$). Solid curves correspond to the exact results, dotted curves correspond to the approximate ones obtained on the basis of Eqs. (13), (12).

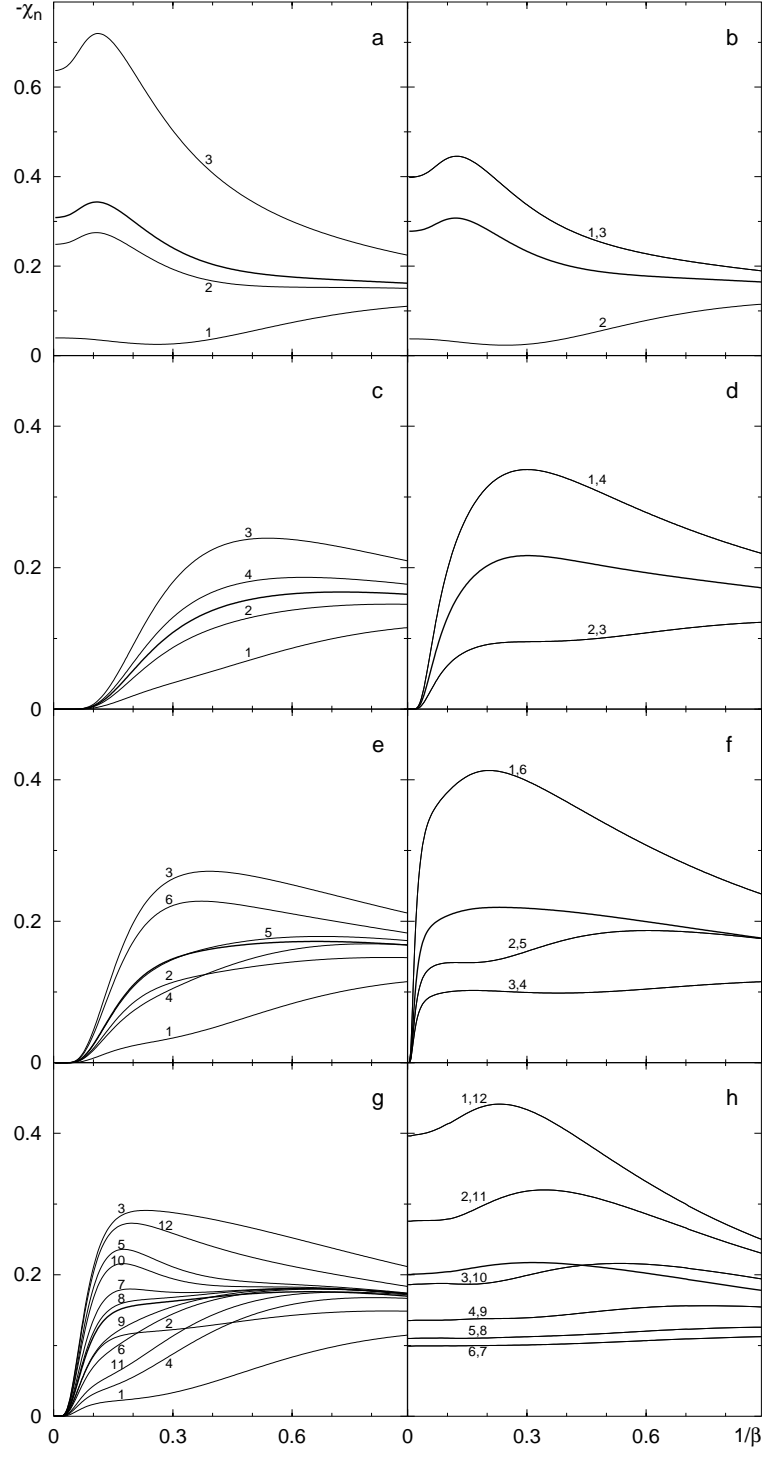


Figure 6: Local static susceptibilities χ_n at $\Omega = 0$ vs. temperature for the chains shown in Fig. 1 ($I = 1$, $\delta = 0.6$). Panel a corresponds to a chain shown in Fig. 1a, panel b corresponds to a chain shown in Fig. 1b, and so on.

6 Summary

To conclude, we studied the local magnetizations and the local static susceptibilities of the spin- $\frac{1}{2}$ XX chain in a transverse field with regularly alternating exchange interactions. These quantities can be calculated exactly using the Jordan–Wigner fermionization, Green function approach and continued fractions. We showed a relation between the alteration of the exchange interactions and i) the zero temperature local magnetizations along the chain at different external fields and ii) the local susceptibilities along the chain at different temperatures. We found that the characteristic fields at which the zero temperature magnetization plateaus start and end up are the same for all sites contrary to the heights of plateaus, which are not universal but site-dependent and which depend on details of intersite interactions and the applied field. We interpreted the observed magnetization profiles from a viewpoint of the strong-coupling approach demonstrating a region of validity of that approximation. We discussed the temperature behavior of the local susceptibilities.

The present study was supported by the DFG (projects 436 UKR 17/2/00 and Ri 615/6–1). O. D. acknowledges the kind hospitality of the Magdeburg University in the summer of 2000 when this paper was completed.

References

- [1] J. P. de Lima and L. L. Gonçalves, J. Magn. Magn. Mater. **206**, 135 (1999).
- [2] M. Nishino, H. Onishi, K. Yamaguchi, and S. Miyashita, preprint cond-mat/0002082.
- [3] D. C. Jonston, R. K. Kremer, M. Troyer, X. Wang, A. Klümper, S. L. Bud’ko, A. F. Panchula, and P. C. Canfield, to be published in Phys. Rev. B (preprint cond-mat/0003271).
- [4] M. Oshikawa, M. Yamanaka, and I. Affleck, Phys. Rev. Lett. **78**, 1984 (1997).
- [5] K. Hida, J. Phys. Soc. Jpn. **63**, 2359 (1994);
K. Okamoto, Solid State Commun. **98**, 245 (1996);
K. Okamoto and A. Kitazawa, J. Phys. A **32**, 4601 (1999);
A. Kitazawa and K. Okamoto, J. Phys.: Condens. Matter **11**, 9765 (1999);
W. Chen, K. Hida, and B. C. Sanctuary, preprint cond-mat/0005544;
W. Chen, K. Hida, and H. Nakano, J. Phys. Soc. Jpn. **68**, 625 (1999).
- [6] D. C. Cabra and M. D. Grynberg, Phys. Rev. B **59**, 119 (1999).

- [7] A. Fledderjohann, C. Gerhardt, M. Karbach, K.-H. Mütter, and R. Wießner, Phys. Rev. B **59**, 991 (1999);
R. M. Wießner, A. Fledderjohann, K.-H. Mütter, and M. Karbach, Eur. Phys. J. B **15**, 475 (2000).
- [8] K. Totsuka, Phys. Rev. B **57**, 3454 (1998);
K. Totsuka, Eur. Phys. J. B **5**, 705 (1998);
A. Honecker, Phys. Rev. B **59**, 6790 (1999);
D. C. Cabra, A. De Martino, A. Honecker, P. Pujol, and P. Simon, Phys. Lett. A **268**, 418 (2000).
- [9] D. C. Cabra, A. Honecker, and P. Pujol, Phys. Rev. Lett. **79**, 5126 (1997);
D. C. Cabra, A. Honecker, and P. Pujol, Phys. Rev. B **58**, 6241 (1998);
F. Mila, Eur. Phys. J. B **6**, 201 (1998);
K. Tandon, S. Lal, S. K. Pati, S. Ramasesha, and D. Sen, Phys. Rev. B **59**, 396 (1999);
A. Furusaki and S.-C. Zhang, Phys. Rev. B **60**, 1175 (1999).
- [10] O. Derzhko, J. Richter, and O. Zaburannyi, Phys. Lett. A **262**, 217 (1999);
O. Derzhko, J. Richter, and O. Zaburannyi, Physica A **282**, 495 (2000).
- [11] Y. Fagot-Revurat, M. Horvatić, C. Berthier, P. Ségransan, G. Dhalenne, and A. Revcolevschi, Phys. Rev. Lett. **77**, 1861 (1996);
M. Horvatić, Y. Fagot-Revurat, C. Berthier, G. Dhalenne, and A. Revcolevschi, Phys. Rev. Lett. **83**, 420 (1999).
- [12] F. Tedoldi, R. Santachiara, and M. Horvatić, Phys. Rev. Lett. **83**, 412 (1999);
F. Alet and E. S. Sørensen, preprint cond-mat/0006282.
- [13] D. N. Zubarev, Usp. Fiz. Nauk **71**, 71 (1960) (in Russian);
D. N. Zubarev, Njėravnovjesnaja statistichjeskaja tjermodinamika, Nauka, Moskva, 1971 (in Russian).